Generalized Digital Redesign Method for Linear Feedback System Based on N-Delay Control

Hiroshi Fujimoto, *Student Member, IEEE,* Atsuo Kawamura, *Senior Member, IEEE,* and Masayoshi Tomizuka, *Fellow, IEEE*

***Abstract*— A new digital redesign method is proposed for feedback control systems, by which the states in the continuous-time system are completely reserved in the redesigned sampled-data system. The features of the proposed method are: 1) the N-delay control is employed, and the lth plant input is changed N_l times during one sampling period; 2) the states of the redesigned sampled-data system completely match those of the original continuous-time closed-loop system at every sampling period; and 3) the proposed redesign method can be applicable for a static state-feedback and/or a dynamic controller. An illustrative example of position control using a dc servo motor is presented. The advantages of the proposed redesign approach are demonstrated both in the time and frequency domains.**

***Index Terms*—Digital control, digital redesign, multirate sampling control, N-delay control.**

I. Introduction

OWING TO THE recent developments in computer and interface hardware, digital controllers are usually utilized for controlling robots or motors because of cost, reliability, flexibility, compactness, and so on.

The digital redesign is a technique by which an analog controller designed in continuous time is converted to an equivalent digital controller [1]. It is, in general, very difficult to let the states of the digital system match those of the original continuous-time system.

Historically, one of the most popular digital redesign methods is the Tustin (or bilinear) transformation, in which an s-domain analog controller is transformed to a z-domain digital controller by

$$s = \frac{2(z-1)}{T(z+1)}. \tag{1}$$

This approach is straightforward, and the stable poles of the controller in the s-domain are mapped inside of the unit circle in the z-domain. However, the closed-loop stability is not assured. Therefore, in this approach, the feedback system may become unstable if the sampling time is set too large.

In [1]–[3], the digital redesign methods based on the closed-loop characteristics were developed. However, these attempts did not assure the closed-loop stability, because approximations were assumed for obtaining solutions of the digital redesign (see Section II). In [4], the feedforward and feedback gains are altered at every sampling period, so that the states of the two systems match at the end of N sampling periods. The method in [4] is similar to the proposed method only in some special cases. However, the number of times of gain alternation, N, is redundant compared to the proposed method in this paper.

The method in [1] was further investigated in [5], and a different approximation was proposed for obtaining a solution of the digital redesign, in which the closed-loop stability was maintained. However, the transition matrices of the original and approximately redesigned systems are not the same. Furthermore, the methods in [1]–[5] have a limitation, in that the original continuous-time controller must be of static state-feedback type and all of the plant state variables must be directly detected.

The other digital redesign methods for a dynamic controller were developed in [6]–[8]. These methods tried to match closed-loop frequency response approximately. However, because of using these approximations, the closed-loop stability could not be assured [6], [7], or the solution of the digital redesign could not be obtained in a large sampling period [8].

Multirate digital controls have been proposed for applications on the pole/zero assignment problem, strong stabilization, simultaneous stabilization, adaptive control, and so on [9]. However, this paper makes the first attempt to apply the multirate digital control to the digital redesign problem.

The purpose of the proposed method is to develop a new digital controller from the analog controller so that all of the states of the sampled-data closed-loop system completely match those of the original continuous-time closed-loop system at every sampling instance. Thus, the stability of the closed-loop system is retained, and the transition matrices of the two systems become identical. In the proposed method, the multirate-input digital control is employed, and the lth plant input is changed N_l times during one sampling period [10]. References [11] and [12] called this method N-delay control, after [13]. The digital redesigned controller can be automatically calculated following the proposed procedure. Moreover, the redesign method for an observer is also presented, in which the multirate-output digital control is employed. Therefore, the proposed method can deal with the system even if a part of the plant states is not directly detected. The proposed digital redesign method is applicable both to a continuous-time static

Manuscript received November 21, 1997; revised January 5, 1999. Recommended by Technical Editor K. Ohnishi.

H. Fujimoto is with the Department of Electrical Engineering, University of Tokyo, Tokyo 113-8656, Japan.

A. Kawamura is with the Department of Electrical and Computer Engineering, Yokohama National University, Yokohama 240-8501, Japan.

M. Tomizuka is with the Department of Mechanical Engineering, University of California, Berkeley, CA 94720-1740 USA.

Publisher Item Identifier S 1083-4435(99)04809-7.

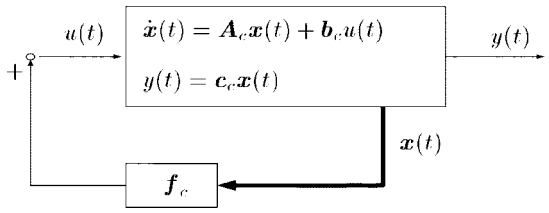

Fig. 1. Continuous-time state-feedback control system.

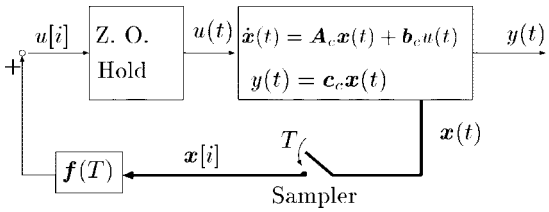

Fig. 2. Discrete-time state-feedback control system.

state-feedback controller and a dynamic controller.

II. Problem of Digital Redesign by Complete State Matching

In this section, we consider the problem of matching the responses of an existing continuous-time system shown in Fig. 1, with those of the discrete-time system shown in Fig. 2 for the same initial conditions. Consider the linear continuous-time system described by

$$\dot{\boldsymbol{x}}(t) = \boldsymbol{A}_c\boldsymbol{x}(t) + \boldsymbol{b}_c u(t). \tag{2}$$

Also, let the continuous-time state-feedback control law be

$$u(t) = \boldsymbol{f}_c\boldsymbol{x}(t). \tag{3}$$

The continuous-time closed-loop system becomes

$$\dot{\boldsymbol{x}}(t) = (\boldsymbol{A}_c + \boldsymbol{b}_c\boldsymbol{f}_c)\boldsymbol{x}(t) \tag{4}$$

and its sampled-data system with the sampling period T is

$$\boldsymbol{x}((i+1)T) = e^{(\boldsymbol{A}_c+\boldsymbol{b}_c\boldsymbol{f}_c)T}\boldsymbol{x}(iT). \tag{5}$$

Consider the discrete-time system utilizing a zero-order hold described by

$$\boldsymbol{x}[i+1] = \boldsymbol{A}\boldsymbol{x}[i] + \boldsymbol{b}u[i] \tag{6}$$

where $\boldsymbol{x}[i] = \boldsymbol{x}(iT), \boldsymbol{A} \triangleq e^{\boldsymbol{A}_c T}$, and $\boldsymbol{b} \triangleq \int_0^T e^{\boldsymbol{A}_c\tau}\,d\tau\boldsymbol{b}_c$. Letting the discrete-time state-feedback control law be $u[i] = \boldsymbol{f}(T)\boldsymbol{x}[i]$, the discrete-time closed-loop system becomes

$$\boldsymbol{x}[i+1] = (\boldsymbol{A} + \boldsymbol{b}\boldsymbol{f}(T))\boldsymbol{x}[i]. \tag{7}$$

From (5) and (7), the digital redesign problem is to find the discrete-time gain $\boldsymbol{f}(T)$ from the continuous-time gain $\boldsymbol{f}_c$ so that the equation

$$\boldsymbol{A} + \boldsymbol{b}\boldsymbol{f}(T) = e^{(\boldsymbol{A}_c+\boldsymbol{b}_c\boldsymbol{f}_c)T} \tag{8}$$

is satisfied. If the above condition is satisfied, the states of the digitally controlled system in (7) completely match those of the continuous-time system in (5) at every sampling period T. The existence of $\boldsymbol{f}(T)$ in (8), however, is not always guaranteed, because the dimension of the input is generally less than that of the state. Therefore, in [1] and [2], (8) is approximately solved for $\boldsymbol{f}(T)$, but, because of the approximation, the stability of the obtained digital closed-loop system is not always assured, and the time response is different from that of the continuous-time feedback system.

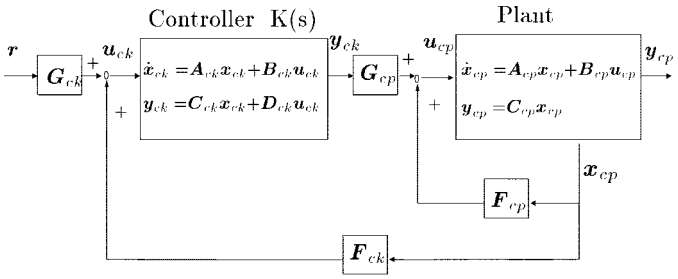

Fig. 3. Continuous-time control system.

III. Digital Redesign by N-Delay Control

In this section, a new digital redesign method by the N-delay input control is presented, in which the lth plant input is changed N_l times during one sampling period. The introduction of the N-delay input control causes the increase of the input dimension, thus, (8) can be solved without any approximation. Moreover, the proposed method is applicable either to a continuous-time dynamic controller or a static state-feedback controller. The proposed method succeeds in this generalization by the introduction of: 1) the closed-loop augmented system consisting of the plant and the dynamic controller and 2) the N-delay input control.

Consider the continuous-time plant described by

$$\dot{\boldsymbol{x}}_{cp}(t) = \boldsymbol{A}_{cp}\boldsymbol{x}_{cp}(t) + \boldsymbol{B}_{cp}\boldsymbol{u}_{cp}(t) \tag{9}$$

$$\boldsymbol{y}_{cp}(t) = \boldsymbol{C}_{cp}\boldsymbol{x}_{cp}(t) \tag{10}$$

where the plant state $\boldsymbol{x}_{cp} \in \boldsymbol{R}^{n_p}$, the plant input $\boldsymbol{u}_{cp} \in \boldsymbol{R}^{m_p}$, and the plant output $\boldsymbol{y}_{cp} \in \boldsymbol{R}^{p_p}$. As shown in Fig. 3, let the continuous-time control law using a state-feedback and/or dynamic controller be

$$\boldsymbol{u}_{cp}(t) = \boldsymbol{F}_{cp}\boldsymbol{x}_{cp}(t) + \boldsymbol{G}_{cp}\boldsymbol{y}_{ck}(t) \tag{11}$$

where the dynamic controller's output $\boldsymbol{y}_{ck} \in \boldsymbol{R}^{p_k}$. Let the dynamic controller $K(s)$ be represented by

$$\dot{\boldsymbol{x}}_{ck}(t) = \boldsymbol{A}_{ck}\boldsymbol{x}_{ck}(t) + \boldsymbol{B}_{ck}\boldsymbol{u}_{ck}(t) \tag{12}$$

$$\boldsymbol{y}_{ck}(t) = \boldsymbol{C}_{ck}\boldsymbol{x}_{ck}(t) + \boldsymbol{D}_{ck}\boldsymbol{u}_{ck}(t) \tag{13}$$

where the dynamic controller's state $\boldsymbol{x}_{ck} \in \boldsymbol{R}^{n_k}$, input $\boldsymbol{u}_{ck} \in \boldsymbol{R}^{m_k}$. Let the controller's input be given by

$$\boldsymbol{u}_{ck}(t) = \boldsymbol{F}_{ck}\boldsymbol{x}_{cp}(t) + \boldsymbol{G}_{ck}\boldsymbol{r}(t) \tag{14}$$

where the reference input $\boldsymbol{r} \in \boldsymbol{R}^{m_r}$ is piecewise constant, i.e., $\boldsymbol{r}(t) = \boldsymbol{r}(iT)$ for $iT \le t < (i+1)T$. From (9) to (14), the continuous-time closed-loop augmented system consisting of the plant and the dynamic controller is represented by

$$\dot{\overline{\boldsymbol{x}}}_c(t) = \overline{\boldsymbol{A}}_c\overline{\boldsymbol{x}}_c(t) + \overline{\boldsymbol{B}}_c\boldsymbol{r}(t) \tag{15}$$

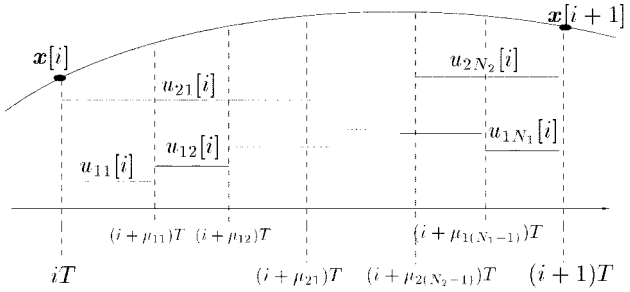

Fig. 4. N-delay input control.

where

$$\overline{\boldsymbol{A}}_c \triangleq \begin{bmatrix} \boldsymbol{A}_{cp}+\boldsymbol{B}_{cp}\boldsymbol{F}_{cp}+\boldsymbol{B}_{cp}\boldsymbol{G}_{cp}\boldsymbol{D}_{ck}\boldsymbol{F}_{ck} & \boldsymbol{B}_{cp}\boldsymbol{G}_{cp}\boldsymbol{C}_{ck} \\ \boldsymbol{B}_{ck}\boldsymbol{F}_{ck} & \boldsymbol{A}_{ck} \end{bmatrix}$$
$$\overline{\boldsymbol{B}}_c \triangleq \begin{bmatrix} \boldsymbol{B}_{cp}\boldsymbol{G}_{cp}\boldsymbol{D}_{ck}\boldsymbol{G}_{ck} \\ \boldsymbol{B}_{ck}\boldsymbol{G}_{ck} \end{bmatrix}$$
$$\overline{\boldsymbol{x}}_c \triangleq \begin{bmatrix} \boldsymbol{x}_{cp} \\ \boldsymbol{x}_{ck} \end{bmatrix} \tag{16}$$

and the sampled-data system for the sampling period T becomes

$$\overline{\boldsymbol{x}}_c((i+1)T) = \overline{\boldsymbol{A}}\overline{\boldsymbol{x}}_c(iT) + \overline{\boldsymbol{B}}\boldsymbol{r}(iT) \tag{17}$$

where

$$\overline{\boldsymbol{A}} \triangleq e^{\overline{\boldsymbol{A}}_c T} \triangleq \begin{matrix} \\ n_p \\ n_k \end{matrix} \begin{matrix} \begin{matrix} n_p & n_k \end{matrix} \\ \begin{bmatrix} \overline{\boldsymbol{A}}_{11} & \overline{\boldsymbol{A}}_{12} \\ \overline{\boldsymbol{A}}_{21} & \overline{\boldsymbol{A}}_{22} \end{bmatrix} \end{matrix} \tag{18}$$

$$\overline{\boldsymbol{B}} \triangleq \int_0^T e^{\overline{\boldsymbol{A}}_c\tau}\overline{\boldsymbol{B}}_c\, d\tau \triangleq \begin{matrix} \\ n_p \\ n_k \end{matrix} \begin{matrix} m_r \\ \begin{bmatrix} \overline{\boldsymbol{B}}_1 \\ \overline{\boldsymbol{B}}_2 \end{bmatrix} \end{matrix}. \tag{19}$$

The redesigned digital control system is required for the exact matching of the states $\overline{\boldsymbol{x}}_c$ at every sampling instant. In the N-delay control, the lth $(l=1,2,\cdots,m_p)$ plant input is changed N_l times during one sampling period, as shown in Fig. 4. $(N_1,\cdots,N_{m_p})$ are referred to as input multiplicities [10]. The selections of the N_l are made by the following condition:

$$N_l \geq \sigma_l \tag{20}$$

where $(\sigma_1,\cdots,\sigma_{m_p})$ are a set of generalized controllability indexes of $(\boldsymbol{A}_{cp},\boldsymbol{B}_{cp})$ which are introduced by authors of [14], and which are defined as follows.

Definition 1: Generalized controllability indexes of $(\boldsymbol{A}_{cp},\boldsymbol{B}_{cp})$ are defined as follows. If $(\boldsymbol{A}_{cp},\boldsymbol{B}_{cp})$ is a controllable pair, n_p linearly independent vectors can be selected from

$$\{\boldsymbol{b}_{c1},\cdots,\boldsymbol{b}_{cm_p},\boldsymbol{A}_{cp}\boldsymbol{b}_{c1},\cdots,\boldsymbol{A}_{cp}\boldsymbol{b}_{cm_p},\cdots,\boldsymbol{A}_{cp}^{n_p-1}\boldsymbol{b}_{cm_p}\}$$

where $\boldsymbol{B}_{cp}=[\boldsymbol{b}_{c1},\cdots,\boldsymbol{b}_{cm_p}]$. Letting φ be a set of these n_p vectors, σ_l are defined by

$$\sigma_l = \text{number}\,\{k|\boldsymbol{A}_{cp}^{k-1}\boldsymbol{b}_{cl}\in\varphi\} \tag{21}$$

$$\sum_{l=1}^{m_p}\sigma_l = n_p. \tag{22}$$

In the case of the single-input plant $(m_p=1)$, this index is simply the same number as the plant order $(\sigma_1=n_p)$. The above definition includes that of Kronecker invariants or controllability indexes defined in [10].

The discrete-time plant using N-delay input control is given by

$$\boldsymbol{x}_{dp}[i+1] = \boldsymbol{A}_{dp}\boldsymbol{x}_{dp}[i] + \sum_{l=1}^{m_p}\sum_{j=1}^{N_l}\boldsymbol{b}_{lj}u_{lj}[i] \tag{23}$$

where $\boldsymbol{x}_{dp}\in\boldsymbol{R}^{n_p}$ is the plant state, $u_{lj}[i]\in\boldsymbol{R}^1$ is the lth plant input for $(i+\mu_{l(j-1)})T\leq t<(i+\mu_{lj})T$ $(l=1,\cdots,m_p, j=1,\cdots,N_l)$, and

$$\boldsymbol{A}_{dp} \triangleq e^{\boldsymbol{A}_{cp}T}$$
$$\boldsymbol{b}_{lj} \triangleq \int_{(1-\mu_{lj})T}^{(1-\mu_{l(j-1)})T} e^{\boldsymbol{A}_{cp}\tau}\boldsymbol{b}_{cl}\, d\tau, \tag{24}$$
$$0=\mu_{l0}<\mu_{l1}<\mu_{l2}<\cdots<\mu_{lN_l}=1. \tag{25}$$

As shown in Fig. 5, let the dynamics of the discrete-time controller be

$$\boldsymbol{x}_{dk}[i+1] = \boldsymbol{L}_1\boldsymbol{x}_{dp}[i] + \boldsymbol{L}_2\boldsymbol{x}_{dk}[i] + \boldsymbol{L}_3\boldsymbol{r}[i] \tag{26}$$

where the discrete-time dynamic controller's state $\boldsymbol{x}_{dk}\in\boldsymbol{R}^{n_k}$. Let the discrete-time control law be

$$\boldsymbol{u}_{lj}[i] = \boldsymbol{f}_{lj}\boldsymbol{x}_{dp}[i] + \boldsymbol{g}_{lj}\boldsymbol{x}_{dk}[i] + \boldsymbol{h}_{lj}\boldsymbol{r}[i]. \tag{27}$$

From (23) to (27), the discrete-time closed-loop augmented system is represented by

$$\overline{\boldsymbol{x}}_d[i+1] = \overline{\boldsymbol{A}}_d\overline{\boldsymbol{x}}_d[i] + \overline{\boldsymbol{B}}_d\boldsymbol{r}[i] \tag{28}$$

where

$$\overline{\boldsymbol{A}}_d \triangleq \begin{bmatrix} \boldsymbol{A}_{dp}+\boldsymbol{B}\boldsymbol{F} & \boldsymbol{B}\boldsymbol{G} \\ \boldsymbol{L}_1 & \boldsymbol{L}_2 \end{bmatrix}$$
$$\overline{\boldsymbol{B}}_d \triangleq \begin{bmatrix} \boldsymbol{B}\boldsymbol{H} \\ \boldsymbol{L}_3 \end{bmatrix}, \quad \overline{\boldsymbol{x}}_d \triangleq \begin{bmatrix} \boldsymbol{x}_{dp} \\ \boldsymbol{x}_{dk} \end{bmatrix} \tag{29}$$
$$\boldsymbol{B} \triangleq [\boldsymbol{b}_{11},\cdots,\boldsymbol{b}_1N_1,\boldsymbol{b}_{21},\cdots,\boldsymbol{b}_{m_pN_{m_p}}] \qquad (n_p\times N)$$
$$\boldsymbol{F} \triangleq [\boldsymbol{f}_{11}^T,\cdots,\boldsymbol{f}_{1N_1}^T,\boldsymbol{f}_{21}^T,\cdots,\boldsymbol{f}_{m_pN_{m_p}}^T]^T \qquad (N\times n_p)$$
$$\boldsymbol{G} \triangleq [\boldsymbol{g}_{11}^T,\cdots,\boldsymbol{g}_{1N_1}^T,\boldsymbol{g}_{21}^T,\cdots,\boldsymbol{g}_{m_pN_{m_p}}^T]^T \qquad (N\times n_k)$$
$$\boldsymbol{H} \triangleq [\boldsymbol{h}_{11}^T,\cdots,\boldsymbol{h}_{1N_1}^T,\boldsymbol{h}_{21}^T,\cdots,\boldsymbol{h}_{m_pN_{m_p}}^T]^T \qquad (N\times m_r)$$
$$N \triangleq N_1+N_2+\cdots+N_{m_p}\geq n_p.$$

Comparing (17) and (28), if the following conditions are satisfied, the states of the digitally controlled system $(\overline{\boldsymbol{x}}_c)$ completely match the states of the continuous-time system $(\overline{\boldsymbol{x}}_d)$ at every sampling period:

$$\begin{bmatrix} \overline{\boldsymbol{A}}_{11} & \overline{\boldsymbol{A}}_{12} \\ \overline{\boldsymbol{A}}_{21} & \overline{\boldsymbol{A}}_{22} \end{bmatrix} = \begin{bmatrix} \boldsymbol{A}_{dp}+\boldsymbol{B}\boldsymbol{F} & \boldsymbol{B}\boldsymbol{G} \\ \boldsymbol{L}_1 & \boldsymbol{L}_2 \end{bmatrix} \tag{30}$$
$$\begin{bmatrix} \overline{\boldsymbol{B}}_1 \\ \overline{\boldsymbol{B}}_2 \end{bmatrix} = \begin{bmatrix} \boldsymbol{B}\boldsymbol{H} \\ \boldsymbol{L}_3 \end{bmatrix}. \tag{31}$$

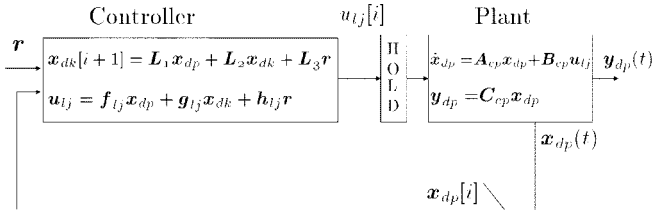

Fig. 5. Discrete-time control system.

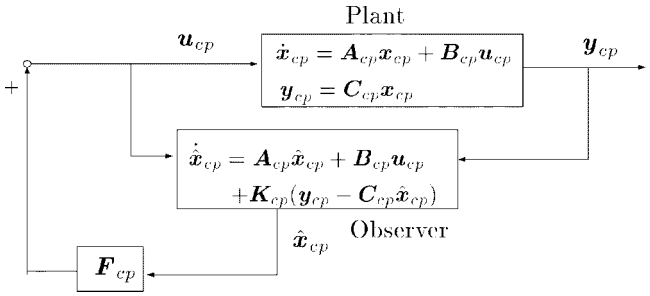

Fig. 6. Continuous-time observer.

Here, the necessary and sufficient condition for solution of the linear matrix equation $(\boldsymbol{Ax} = \boldsymbol{b})$ is

$$\operatorname{rank} \boldsymbol{A} = \operatorname{rank} [\boldsymbol{A}, b]. \tag{32}$$

Therefore, the necessary and sufficient conditions for the existence of $\boldsymbol{F}, \boldsymbol{G}, \boldsymbol{H}$ in (30) and (31) are given by

$$\begin{aligned} \operatorname{rank} \boldsymbol{B} &= \operatorname{rank} [\boldsymbol{B}, \overline{\boldsymbol{A}}_{11} - \boldsymbol{A}_{dp}] \\ &= \operatorname{rank} [\boldsymbol{B}, \overline{\boldsymbol{A}}_{12}] = \operatorname{rank} [\boldsymbol{B}, \overline{\boldsymbol{B}}_1]. \end{aligned} \tag{33}$$

Concerning the matrix $\boldsymbol{B}$, the next theorem is proved in [14], if σ_l is the generalized controllability index. In the case of the controllability index, it is also proved in [10].

Theorem 1: Let $(\boldsymbol{A}_{cp}, \boldsymbol{B}_{cp})$ be a controllable pair. If the input multiplicities satisfy $N_l \geq \sigma_l$ for $(l = 1, 2, \cdots, m_p)$, for almost all μ_{lj} $(l = 1, 2, \cdots, m_p, j = 1, \cdots, N_l - 1)$ and almost all T, the matrix $\boldsymbol{B}$ has full row rank, i.e.,

$$\operatorname{rank} \boldsymbol{B} = n_p. \tag{34}$$

Because of this theorem, the row rank $\boldsymbol{B}$ in (33) is full, thus, (33) is satisfied. As a result, the existence of $\boldsymbol{F}, \boldsymbol{G}, \boldsymbol{H}$ in (30) and (31) is assured. Solving (30) and (31), the redesigned parameters are given by

$$\begin{aligned} \boldsymbol{F} &= \boldsymbol{B}^{-}(\overline{\boldsymbol{A}}_{11} - \boldsymbol{A}_{dp}) \\ \boldsymbol{G} &= \boldsymbol{B}^{-}\overline{\boldsymbol{A}}_{12} \\ \boldsymbol{H} &= \boldsymbol{B}^{-}\overline{\boldsymbol{B}}_1 \\ \boldsymbol{L}_1 &= \overline{\boldsymbol{A}}_{21} \\ \boldsymbol{L}_2 &= \overline{\boldsymbol{A}}_{22} \\ \boldsymbol{L}_3 &= \overline{\boldsymbol{B}}_2 \end{aligned} \tag{35}$$

where $\boldsymbol{B}^{-}$ is the generalized inverse of matrix $\boldsymbol{B}$ [15].

Comments: 1) if $(\boldsymbol{A}_{cp}, \boldsymbol{B}_{cp})$ is a controllable pair, the system, which is controlled by either a continuous-time dynamic controller or a static state-feedback controller, can be always redesigned in this method; 2) if the original continuous-time system is stably designed, the redesigned system is assured to be stable because the two transition matrices (30) become identical. Moreover, (30) can guarantee the intersample stability [16]; and 3) the states of the redesigned sampled-data system completely match those of the original continuous-time closed-loop system at every sampling period, independent of sampling period. Therefore, the proposed method is superior to the conventional method, such as Tustin transformation, and other methods [1]–[8].

IV. Digital Redesign for Observer

Because the redesigned control laws obtained in Section III are state-feedback control, as shown in (26) and (27), all states need to be detected directly. However, in the general case, all states are not always detected directly, and the calculation time delay may not be negligible. Therefore, in this section, the discrete-time state observer is considered to feed back the estimated plant state $\hat{\boldsymbol{x}}[i]$ instead of the plant state $\boldsymbol{x}[i]$.

In this section, the digital redesign method for the state observer which is based on the multirate-output sampling is proposed by using the duality of the redesign method for the controller.

Consider the designed continuous-time observer shown in Fig. 6 for the continuous-time plant (9) described by

$$\dot{\hat{\boldsymbol{x}}}_{cp}(t) = \boldsymbol{A}_{cp}\hat{\boldsymbol{x}}_{cp}(t) + \boldsymbol{B}_{cp}\boldsymbol{u}_{cp}(t) + \boldsymbol{K}_{cp}(\boldsymbol{y}_{cp} - \boldsymbol{C}_{cp}\hat{\boldsymbol{x}}_{cp}(t)) \tag{36}$$

where the estimated plant state is $\hat{\boldsymbol{x}}_{cp}$. Because the estimation error of the continuous-time state $\boldsymbol{e}_{cp}$ becomes

$$\begin{aligned} \dot{\boldsymbol{e}}_{cp}(t) &= \dot{\boldsymbol{x}}_{cp}(t) - \dot{\hat{\boldsymbol{x}}}_{cp}(t) \\ &= (\boldsymbol{A}_{cp} - \boldsymbol{K}_{cp}\boldsymbol{C}_{cp})\boldsymbol{e}_{cp}(t). \end{aligned} \tag{37}$$

The sampled-data system for the sampling period T is represented by

$$\boldsymbol{e}_{cp}((i+1)T) = e^{(\boldsymbol{A}_{cp} - \boldsymbol{K}_{cp}\boldsymbol{C}_{cp})T}\boldsymbol{e}_{cp}(iT). \tag{38}$$

In the proposed method, the multirate-output sampling control is employed, in which the qth plant output is detected M_q times during one sampling period, as shown in Fig. 7, and the discrete-time estimation errors $(\boldsymbol{e}_{dp})$ completely match the continuous-time estimation errors $(\boldsymbol{e}_{cp})$ at every sampling period. This period is also called the frame period [17]. This control is a duality scheme of the N-delay input control, and it is also called the M-delay output control. The selections of output multiplicities M_q are made by the following condition.:

$$M_q \geq \rho_q \tag{39}$$

where $(\rho_1, \cdots, \rho_{p_p})$ are a set of generalized observability indexes of $(\boldsymbol{A}_{cp}, \boldsymbol{C}_{cp})$ which are defined as follows.

Definition 2: Generalized observability indexes of $(\boldsymbol{A}_{cp}, \boldsymbol{C}_{cp})$ are defined as follows. If $(\boldsymbol{A}_{cp}, \boldsymbol{C}_{cp})$ is an observable pair, n_p linearly independent vectors can be selected from

$$\{\boldsymbol{c}_{c1}, \cdots, \boldsymbol{c}_{cp_p}, \boldsymbol{c}_{c1}\boldsymbol{A}_{cp}, \cdots, \boldsymbol{c}_{cp_p}\boldsymbol{A}_{cp}, \cdots, \boldsymbol{c}_{cp_p}\boldsymbol{A}_{cp}^{n_p - 1}\}$$

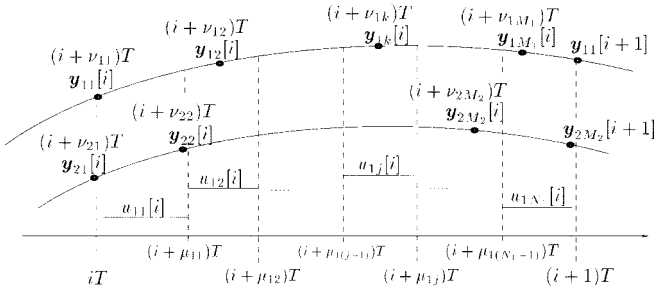

Fig. 7. M-delay output control.

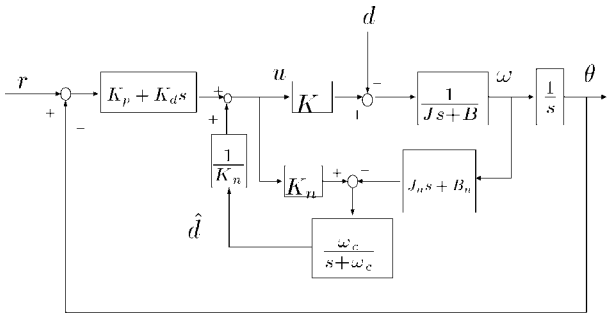

Fig. 8. The position control with the disturbance observer.

where $\boldsymbol{C}_{cp}=[\boldsymbol{c}_{c1}^T,\cdots,\boldsymbol{c}_{cp_p}^T]^T$. Letting φ be a set of these n_p vectors, ρ_q are defined by

$$\rho_q=\text{number}\,\{k|\boldsymbol{c}_{cq}\boldsymbol{A}_{cp}^{k-1}\in\varphi\} \tag{40}$$

$$\sum_{q=1}^{p_p}\rho_q=n_p. \tag{41}$$

The discrete-time plant using N-delay input control and M-delay output control is given by

$$\boldsymbol{x}_{dp}[i+1]=\boldsymbol{A}_{dp}\boldsymbol{x}_{dp}[i]+\sum_{l=1}^{m_p}\sum_{j=1}^{N_l}\boldsymbol{b}_{lj}u_{lj}[i] \tag{42}$$

$$y_{qk}[i]=\boldsymbol{c}_{qk}\boldsymbol{x}_{dp}[i]+\sum_{l=1}^{m_p}\sum_{j=1}^{N_l}d_{qklj}u_{lj}[i] \tag{43}$$

where

$$\boldsymbol{c}_{qk}\triangleq\boldsymbol{c}_{cq}e^{\boldsymbol{A}_{cp}\nu_{qk}T} \tag{44}$$

$$d_{qklj}\triangleq\begin{cases}\mu_{lj}<\nu_{qk}: & \boldsymbol{c}_{cq}\displaystyle\int_{(\nu_{qk}-\mu_{lj})T}^{(\nu_{qk}-\mu_{l(j-1)})T}e^{\boldsymbol{A}_{cp}\tau}\boldsymbol{b}_{cl}\,d\tau\\ \mu_{l(j-1)}<\nu_{qk}\le\mu_{lj}: & \boldsymbol{c}_{cq}\displaystyle\int_{0}^{(\nu_{qk}-\mu_{l(j-1)})T}e^{\boldsymbol{A}_{cp}\tau}\boldsymbol{b}_{cl}\,d\tau\\ \nu_{qk}\le\mu_{l(j-1)}: & 0,\end{cases}$$
$$0\le\nu_{q1}<\nu_{q2}<\cdots<\nu_{qM_q}<1 \tag{45}$$

and $y_{qk}\in\boldsymbol{R}^1$ is the qth plant output on $t=(i+\nu_{qk})T$ $(q=1,2,\cdots,p_p,k=1,2,\cdots,M_q)$.

Using the intersampling outputs y_{qk}, let the discrete-time observer be

$$\begin{aligned}\hat{\boldsymbol{x}}_{dp}[i+1]&=\boldsymbol{A}_{dp}\hat{\boldsymbol{x}}_{dp}[i]+\sum_{l=1}^{m_p}\sum_{j=1}^{N_l}\boldsymbol{b}_{lj}u_{lj}[i]+\sum_{q=1}^{p_p}\sum_{k=1}^{M_q}\\&\quad\cdot\boldsymbol{k}_{qk}\left\{y_{qk}[i]-\left(\boldsymbol{c}_{qk}\hat{\boldsymbol{x}}_{dp}[i]+\sum_{l=1}^{m_p}\sum_{j=1}^{N_l}d_{qklj}u_{lj}[i]\right)\right\}\end{aligned} \tag{46}$$

where the state of the discrete-time observer $\hat{\boldsymbol{x}}_{dp}\in\boldsymbol{R}^{n_p}$. The estimation error of the discrete-time state $\boldsymbol{e}_{dp}$ is represented by

$$\begin{aligned}\boldsymbol{e}_{dp}[i+1]&=\boldsymbol{x}_{dp}[i+1]-\hat{\boldsymbol{x}}_{dp}[i+1]\\&=(\boldsymbol{A}_{dp}-\boldsymbol{KC})\boldsymbol{e}_{dp}[i]\end{aligned} \tag{47}$$

where

$$\begin{aligned}K&\triangleq[\boldsymbol{k}_{11},\cdots,\boldsymbol{k}_{1M_1},\boldsymbol{k}_{21},\cdots,\boldsymbol{k}_{p_pM_{p_p}}]\qquad(n_p\times M)\\C&\triangleq[\boldsymbol{c}_{11}^T,\cdots,\boldsymbol{c}_{1M_1}^T,\boldsymbol{c}_{21}^T,\cdots,\boldsymbol{c}_{p_pM_{p_p}}^T]^T\qquad(M\times n_p)\\M&=M_1+M_2+\cdots+M_{p_p}\ge n_p.\end{aligned} \tag{48}$$

Comparing (38) and (47), if the following condition is satisfied, the estimation errors of the continuous-time states $(\boldsymbol{e}_{cp})$ completely match those of the discrete-time states $(\boldsymbol{e}_{dp})$ at every sampling period:

$$e^{(\boldsymbol{A}_{cp}-\boldsymbol{K}_{cp}\boldsymbol{C}_{cp})T}=\boldsymbol{A}_{dp}-\boldsymbol{KC}. \tag{49}$$

From (32), the necessary and sufficient condition for the existence of $\boldsymbol{K}$ in (49) is given by

$$\text{rank}\,\boldsymbol{C}=\text{rank}\begin{bmatrix}\boldsymbol{C}\\ \boldsymbol{A}_{dp}-e^{(\boldsymbol{A}_{cp}-\boldsymbol{K}_{cp}\boldsymbol{C}_{cp})T}\end{bmatrix}. \tag{50}$$

Concerning the matrix $\boldsymbol{C}$, the next theorem is proved in [14], if ρ_q is the generalized observability controllability index. In the case of the observability index, it is also proved in [17].

Theorem 2: Let $(\boldsymbol{A}_{cp},\boldsymbol{C}_{cp})$ be an observable pair. If the output multiplicities satisfy $M_q\ge\rho_q$ for $(q=1,2,\cdots,p_p)$, for almost all ν_{qk} $(k=1,\cdots,M_q)$ and almost all T, the matrix $\boldsymbol{C}$ has full column rank, i.e.,

$$\text{rank}\,\boldsymbol{C}=n_p. \tag{51}$$

Because of this theorem, the column rank $\boldsymbol{C}$ in (50) is full, thus, (50) is satisfied. As a result, the existence of $\boldsymbol{K}$ in (49) is assured. Solving (49), the redesigned parameters are given by

$$\boldsymbol{K}=(\boldsymbol{A}_{dp}-e^{(\boldsymbol{A}_{cp}-\boldsymbol{K}_{cp}\boldsymbol{C}_{cp})T})\boldsymbol{C}^{-}. \tag{52}$$

In this section, only the redesign method for a full-order observer was presented. However, a minimum-order observer can also be redesigned the same way as above [14].

V. Illustrative Example

A. Digital Redesign of a Position Control System for a DC Servo Motor with the Disturbance Observer

In this section, simulation and experimental results for a position control system for a dc servo motor with the disturbance observer are presented, as shown in Fig. 8.

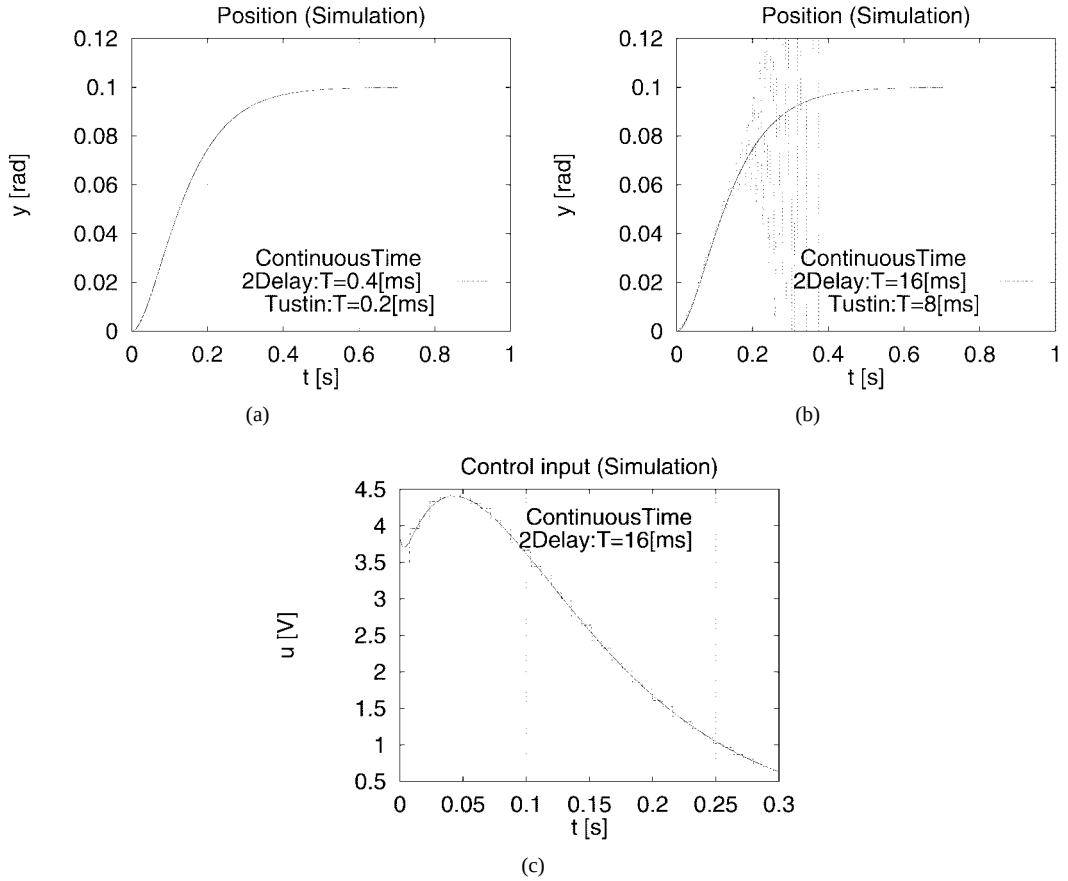

Fig. 9. Simulation results. (a) Position responses ($T_u = 0.2\,[\mathrm{ms}]$). (b) Position responses ($T_u = 8\,[\mathrm{ms}]$). (c) Control input responses ($T_u = 8\,[\mathrm{ms}]$).

In the experiments, a digital signal processor (DSP) (NEC: μPD77230, 32-b floating point) is used, and the 1/100 gear ratio dc servo motor is driven by a 10-kHz switching frequency MOSFET chopper. The pulse counter generates 1000 pulses/rev on the motor shaft (it becomes 100 000 pulses/rev on the geared shaft), and the speed is detected through a 12-b A/D converter by a tachometer [18].

In the design of the continuous-time controller, assuming that the disturbance torque d is a step-function type, the plant is represented by

$$\begin{aligned}\dot{\boldsymbol{x}}_{cp}(t) &= \boldsymbol{A}_{cp}\boldsymbol{x}_{cp}(t) + \boldsymbol{b}_{cp}u_{cp}(t)\\ \boldsymbol{A}_{cp} &= \begin{bmatrix} 0 & 1 & 0 \\ 0 & -\dfrac{B}{J} & -\dfrac{1}{J} \\ 0 & 0 & 0 \end{bmatrix}\\ \boldsymbol{b}_{cp} &= \begin{bmatrix} 0 \\ \dfrac{K}{J} \\ 0 \end{bmatrix}\\ \boldsymbol{x}_{cp} &= \begin{bmatrix} \theta \\ \omega \\ d \end{bmatrix}\end{aligned} \tag{53}$$

where θ is angular position, ω is angular velocity, and u_{cp} is the dc voltage of the motor terminal. Assuming the command input r to be a step-function type, the continuous-time control law is given by

$$\begin{aligned}u_{cp} &= K_p(r-\theta) - K_d\omega + \frac{1}{K_n}\hat{d}\\ &= \boldsymbol{f}_{cp}\hat{\boldsymbol{x}}_{cp} + g_{cp}r\end{aligned} \tag{54}$$

where $\boldsymbol{f}_{cp} = [-K_p, -K_d, (1/K_n)], g_{cp} = K_p, \hat{\boldsymbol{x}}_{cp} = [\theta, \omega, \hat{d}]^T$. As shown in Fig. 8, the continuous-time disturbance observer is also given by

$$\begin{aligned}\dot{\hat{v}}_c(t) &= \hat{A}_c\hat{v}_c(t) + \hat{B}_c\omega(t) + \hat{J}_c u_{cp}(t)\\ \hat{d}(t) &= \hat{v}_c(t) + l_c\omega(t)\end{aligned} \tag{55}$$

where $\hat{A}_c = -\omega_c, \hat{B}_c = -B_n\omega_c + J_n\omega_c^2, \hat{J}_c = K_n\omega_c$, and ω_c is the cutoff frequency of the low-pass filter.

The nominal values of the plant constants are $J_n = 0.0730[\mathrm{kg}\cdot\mathrm{m}^2], B_n = 3.26[\mathrm{kg}\cdot\mathrm{m}^2/\mathrm{s}], K_n = 0.388[\mathrm{N}\cdot\mathrm{m}/\mathrm{V}]$. Also, the continuous-time control parameters are $K_p = 8.91, K_d = -4.99, \omega_c = 300[\mathrm{rad}/\mathrm{s}]$.

First, the control law (54) is redesigned. Although $(\boldsymbol{A}_{cp}, \boldsymbol{B}_{cp})$ in (53) is not controllable, the conditions in (33) are satisfied for input multiplicity $N_1 = 2$. From (35), the redesigned control laws for $T = 0.4\,[\mathrm{ms}], \mu_{11} = 0.5$ are obtained, as follows:

$$\begin{bmatrix} \boldsymbol{u}_{11}[i] \\ \boldsymbol{u}_{12}[i] \end{bmatrix} = \begin{bmatrix} -33.4 & 3.38 & 2.57 \\ -33.6 & 3.34 & 2.57 \end{bmatrix} \begin{bmatrix} \theta[i] \\ \omega[i] \\ \hat{d}[i] \end{bmatrix} + \begin{bmatrix} 33.4 \\ 33.6 \end{bmatrix} \boldsymbol{r}[i].$$

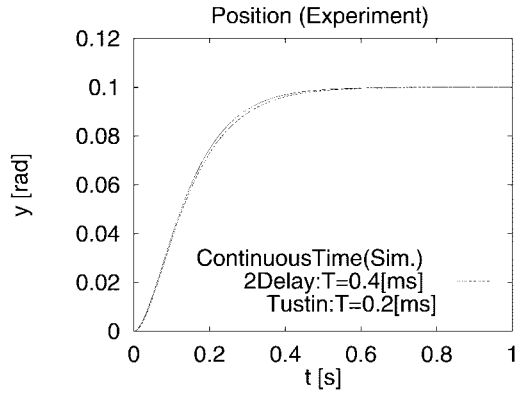

(a)

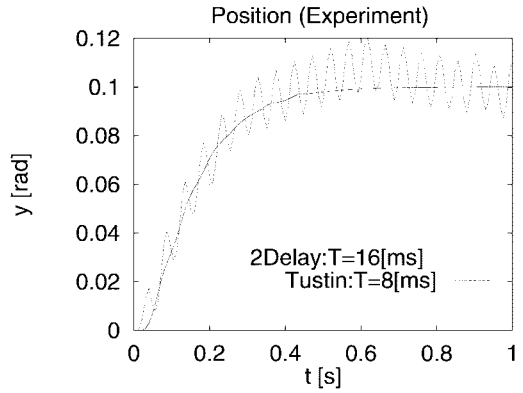

(b)

Fig. 10. Experiment results. (a) Position responses ($T_u = 0.2\,[\mathrm{ms}]$). (b) Position responses ($T_u = 8\,[\mathrm{mss}]$).

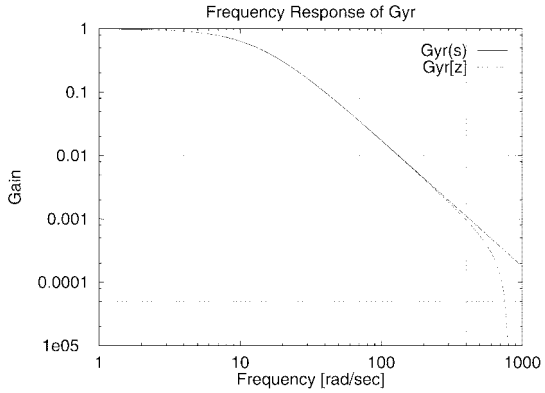

(a)

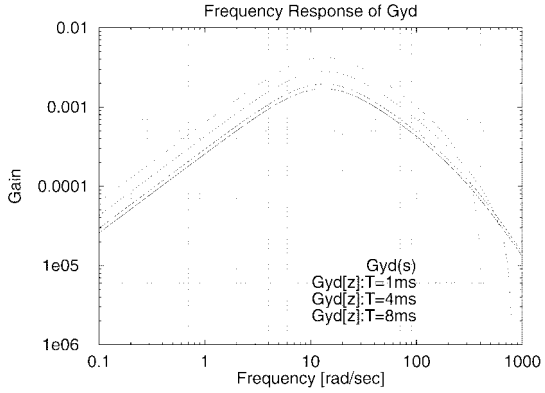

(b)

Fig. 11. Frequency responses. (a) Command responses (G_{yr}). (b) Disturbance responses (G_{yd}).

Second, the disturbance observer in (55) is redesigned the same way as in Section IV. For $T = 0.4\,[\mathrm{ms}], \mu_{11} = 0.5$, the discrete-time observer is obtained [14] by

$$\begin{aligned} \hat{v}_d[i+1] &= \hat{A}_d\hat{v}_d[i] + \hat{B}_d\omega[i] + \hat{J}_{11}u_{11}[i] + \hat{J}_{12}u_{12}[i] \\ \hat{d}[i] &= \hat{v}_d[i] + l_d\omega[i] \end{aligned} \tag{56}$$

where $l_d = -20.8, \hat{A}_d = 0.887, \hat{B}_d = 1.99, \hat{J}_{11} = 2.12 \times 10^{-2}$, and $\hat{J}_{12} = 2.21 \times 10^{-2}$.

B. Simulations and Experiments

Because the redesign system uses the two-delay input control, the output sampling period T is twice as long as the input sampling period T_u. In the following simulations and experiments, the proposed method (two-delay) is compared with the Tustin (bilinear) transformation at the same input sampling period so that the calculation costs of the two systems may be equal and these comparisons may be fair. Therefore, the output sampling period of the proposed method is twice as long as that of the Tustin transformation.

Simulated and experimental results are shown in Figs. 9 and 10. In the very short sampling period (0.2 ms), we find the Tustin transformation and the proposed transformation have almost the same time responses. However, in the long sampling period (8 ms), as shown in Figs. 9 and 10(b), the proposed method gives better performance than the Tustin transformation. While the responses of the Tustin transformation are unstable, those of the proposed method are stable, and exactly match the continuous-time responses.

The simulated time responses of the control input are shown in Fig. 9(c), which indicates that the control input of the proposed method is smooth in spite of using two-delay control.

C. Frequency Responses of the Closed-Loop Systems

The frequency responses from the command input (r) to the plant state (θ) are shown in Fig. 11(a). In the wide frequency band lower than the Nyquist frequency, the discrete-time response redesigned by the proposed method $(G_{yr}[z])$ matches the continuous-time response $(G_{yr}(s))$. That is guaranteed by (17), (28), (30), and (31).

The frequency responses from the disturbance torque (d) to the plant state (θ) are also shown in Fig. 11(b), which indicates that the longer the sampling period is, the poorer the disturbance rejection performance is. Therefore, Fig. 11(b) tells us the practical limitations of the sampling period for the proposed method.

D. Disturbance Responses

The simulation results of the time responses under the step function type disturbances (5 N·m, $t > 1$ s) are shown in Fig. 12. In the short sampling period (0.4 ms), the redesigned

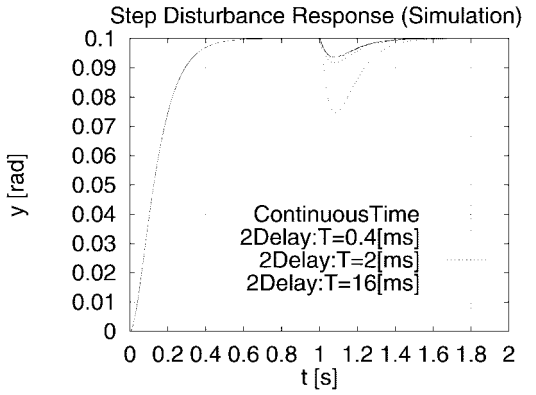

(a)

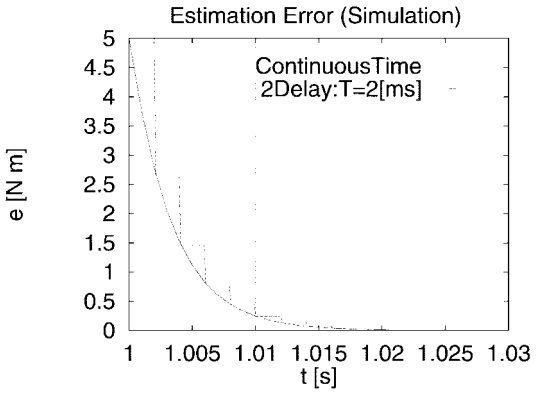

(b)

Fig. 12. Responses under step-type disturbance (simulation). (a) Position responses. (b) Estimation errors of disturbance.

system has almost as same performance as the continuous-time system. However, as mentioned above [Fig. 11(b)], the disturbance rejection performance becomes poor in the large sampling period (16 ms).

The time responses of the disturbance estimation errors are shown in Fig. 12(b). The estimation error of the discrete-time observer which is obtained by the proposed method completely matches that of the continuous-time observer at every sampling period. Fig. 12(b) also assures that there is no offset between the command input (r) and the plant state (θ).

VI. Conclusion

New digital redesign methods, both for a controller and an observer using N-delay control, were proposed. A position control using a dc servo motor was selected for an example, and simulations and experiments were performed, which indicated that the proposed method had better performance than that of the Tustin transformed digital controller. Moreover, the disturbance rejection performance is considered both in the time and frequency domains.

One of the remarkable advantages of the proposed method is that the states of the sampled-data system completely become equal to those of the continuous-time system, independent of sampling period and, as a result, the stability of the redesigned system is assured. The choice of μ_j (a parameter of the input sampling period) should be further investigated for the optimal intersample time responses and the smoothest control inputs.

The proposed method can be extended to be applicable to the output-feedback-type problem, which will be presented at the next opportunity.

References

[1] B. C. Kuo, *Digital Control Systems*. New York: Holt, Rinehart and Winston, 1980.
[2] B. C. Kuo and D. W. Peterson, "Optimal discretization of continuous-data control system," *Automatica*, vol. 9, no. 1, pp. 125–129, 1973.
[3] L. S. Shieh, J. L. Zhang, and S. Ganesan, "Pseudo-continuous-time quadratic regulators with pole in a specific region," *Proc. Inst. Elect. Eng.*, vol. 137, pt. D, no. 5, pp. 297–301, 1990.
[4] R. A. Yackel, B. C. Kuo, and G. Singh, "Digital redesign of continuous systems by matching of states at multiple sampling periods," *Automatica*, vol. 10, no. 1, pp. 105–111, 1974.
[5] L. S. Shieh, X. M. Zhao, and J. L. Zhang, "Locally optimal-digital redesign of continuous-time systems," *IEEE Trans. Ind. Electron.*, vol. 36, pp. 511–515, Aug. 1989.
[6] K. S. Rattan, "Digitalization of continuous control systems," *IEEE Trans. Automat. Contr.*, vol. 29, pp. 282–285, Mar. 1984.
[7] ———, "Compensating for computational delay in digital equivalent of continuous control systems," *IEEE Trans. Automat. Contr.*, vol. 34, pp. 895–899, Aug. 1989.
[8] J. P. Keller and B. D. O. Anderson, "A new approach to the discretization of continuous-time controllers," *IEEE Trans. Automat. Contr.*, vol. 37, pp. 214–223, Feb. 1992.
[9] M. Araki, "Recent developments in digital control theory," in *Proc. IFAC World Congr.*, July 1993, vol. 9, pp. 251–260.
[10] M. Araki and T. Hagiwara, "Pole assignment by multirate-data output feedback," *Int. J. Control*, vol. 44, no. 6, pp. 1661–1673, 1986.
[11] K. L. Moore, S. P. Bhattacharyya, and M. Dahleh, "Capabilities and limitations of multirate control schemes," *Automatica*, vol. 29, no. 4, pp. 941–951, 1993.
[12] H. Fujimoto, A. Kawamura, and M. Tomizuka, "Proposal of generalized digital redesign method in use of N-delay control," in *Proc. Amer. Control Conf.*, June 1997, pp. 3290–3294.
[13] T. Mita, Y. Chida, Y. Kazu, and H. Numasato, "Two-delay robust digital control and its applications—Avoiding the problem on unstable limiting zeros," *IEEE Trans. Automat. Contr.*, vol. 35, pp. 962–970, Aug. 1990.
[14] H. Fujimoto and A. Kawamura, "New digital redesign method in use of N-Delay control (in Japanese)," *Trans. IEEJ*, vol. 117-D, no. 5, pp. 645–654, 1997.
[15] P. Lancaster and M. Tismenetsky, *The Theory of Matrices*. New York: Academic, 1985.
[16] T. Chen and B. Francis, *Optimal Sampled-Data Control Systems*. Berlin, Germany: Springer-Verlag, 1995.
[17] T. Hagiwara and M. Araki, "Design of a state state feedback controller based on the multirate sampling of plant output," *IEEE Trans. Automat. Contr.*, vol. 33, pp. 812–819, Sept. 1988.
[18] A. Kawamura, K. Miura, and T. Ishizwawa, "Observer based sliding mode CP control of two axis scara robot," in *Proc. IEEE Int. Workshop Advanced Motion Control*, Mar. 1990, pp. 197–202.

Hiroshi Fujimoto (S'99) was born in Tokyo, Japan, in 1974. He received the B.S. and M.S. degrees in electrical and computer engineering from Yokohama National University, Yokohama, Japan, in 1996 and 1998, respectively. He is currently working towards the Ph.D. degree in the Department of Electrical Engineering, University of Tokyo, Tokyo, Japan.

He has also been a Research Fellow of the Japan Society for the Promotion of Science since 1998. His interests include control engineering, motion control, and digital control. His current work concerns a multirate sampled-data system for a new digital motion control method.

Mr. Fujimoto is a student member of the Institute of Electrical Engineers of Japan.

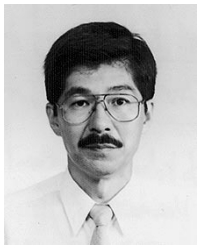

Atsuo Kawamura (S'77–M'78–SM'96) was born in Yamaguchi Prefecture, Japan, in 1953. He received the B.S.E.E., M.S.E.E., and Ph.D. degrees in electrical engineering from the University of Tokyo, Tokyo, Japan, in 1976, 1978, and 1981, respectively.

In 1981, he joined the Department of Electrical and Computer Engineering, University of Missouri, Columbia, as a Postdoctoral Fellow, and was an Assistant Professor there from 1983 to 1986. He joined the Department of Electrical and Computer Engineering, Yokohama National University, Yokohama, Japan, in 1986 as an Associate Professor and, in 1996, he became a Professor. His interests include power electronics, digital control, electric vehicles, robotics, and ultrasonic actuators. He will serve as the Technical Program Chairman of the Workshop on Advanced Motion Control in 2000 (AMC2000).

Prof. Kawamura received the IEEE TRANSACTIONS ON INDUUSTRY APPLICATIONS Prize Paper Award in 1988 and the Prize Paper Award from the Institute of Electrical Engineers of Japan (IEEJ) in 1996. He was the Conference Chairperson of the IEEE Industry Applications Society and IEEJ Industry Applications Society Joint Power Conversion Conference (PCC-Yokohama) in 1993. He served as the Technical Program Chairman of the IEEE Power Electronics Specialist Conference (PESC'98) in 1998. He has been an Associate Editor of the IEEE TRANSACTIONS ON POWER ELECTRONICS since 1995. He is a member of the IEEJ, Robotics Society of Japan, Institute of Electronics, Information and Communication Engineers, and Society of Instrument and Control Engineering.

Masayoshi Tomizuka (M'86–SM'95–F'97), for a photograph and biography, see p. 24 of the March 1999 issue of this TRANSACTIONS.